The extended main-sequence turn-off cluster NGC 1856: rotational evolution in a coeval stellar ensemble

F. D'Antona,[1][*] M. Di Criscienzo,[1] T. Decressin,[1] A. P. Milone,[2] E. Vesperini[3] and P. Ventura[1]

[1]*INAF, Osservatorio Astronomico di Roma, Via Frascati 33, I-00040 Monteporzio Catone (Roma), Italy*
[2]*Research School of Astronomy & Astrophysics, Australian National University, Canberra, ACT 2611, Australia*
[3]*Department of Astronomy, Indiana University, Swain West, 727 E. 3rd Street, Bloomington, IN 47405, USA*

ABSTRACT

Multiple or extended turn-offs in young clusters in the Magellanic Clouds have recently received large attention. A number of studies have shown that they may be interpreted as the result of a significant age spread (several 10^8 yr in clusters aged 1–2 Gyr), while others attribute them to a spread in stellar rotation. We focus on the cluster NGC 1856, showing a splitting in the upper part of the main sequence, well visible in the colour $m_{F336W} - m_{F555W}$, and a very wide turn-off region. Using population synthesis available from the Geneva stellar models, we show that the cluster data can be interpreted as superposition of two main populations having the same age (∼350 Myr), composed for 2/3 of very rapidly rotating stars, defining the upper turn-off region and the redder main sequence, and for 1/3 of slowly/non-rotating stars. Since rapid rotation is a common property of the B-A type stars, the main question raised by this model concerns the origin of the slowly/non-rotating component. Binary synchronization is a possible process behind the slowly/non-rotating population; in this case, many slowly/non-rotating stars should still be part of binary systems with orbital periods in the range from 4 to 500 d. For these orbital periods, Roche lobe overflow occurs during the evolution of the primary off the main sequence, so most primaries may not be able to ignite core helium burning, consistently why the lack of a red clump progeny of the slowly rotating population.

Key words: stars: early-type – Hertzsprung–Russell and colour–magnitude diagrams – stars: interiors – globular clusters: general – Magellanic Clouds.

1 INTRODUCTION

Extended main-sequence turn-off regions (eMSTO) appear to be a typical feature of massive intermediate–age globular clusters (GCs) in both Magellanic Clouds, as shown by deep observations of their colour–magnitude diagrams (CMDs) taken with the ACS and WFC3 onboard the *Hubble Space Telescope* (*HST*). Most of these clusters are in the age range 1–2 Gyr (Mackey et al. 2008; Milone et al. 2009), and, if the eMSTOs are interpreted as due to differences in the formation epoch of stars, their age spreads range from 150 to ∼500 Myr (Milone et al. 2009; Girardi, Eggenberger & Miglio 2011; Goudfrooij et al. 2011; Rubele et al. 2013). This possible age spread has been sometimes used (Conroy & Spergel 2011) as a possible evidence of the age difference underlying multiple generations in old galactic GCs (Gratton, Carretta & Bragaglia 2012; Piotto et al. 2012), although theoretical work on GCs shows

that the possible age differences must be contained within about 100 Myr (D'Ercole et al. 2010). Moreover, (limited) spectroscopic observations of stars in the eMSTO cluster NGC 1806 seem to suggest that this cluster has homogeneous abundance of O, Na, Al and Mg, and that the O–Na anticorrelation may be not present in clusters with extended turnoffs (Mucciarelli et al. 2014). If confirmed by larger data set of spectroscopic studies in clusters having eMSTO, the result would indicate the lack of any connection between eMSTO clusters and multiple-populations GCs, since the anticorrelation between oxygen and sodium abundances is one of the key fingerprints of multiple populations in old GCs. Notice that, in galactic GCs, the Na–O anticorrelation is present also at metallicities as large as those of LMC clusters, in which oxygen is slightly depleted, but the sodium abundance spans >0.5 dex (Carretta et al. 2009). Other LMC intermediate age clusters may have sodium spreads by 0.1–0.35 dex, which may hint to a possible link with the presence of second-generation stars (see the discussion in Goudfrooij et al. 2014), but the data (Mucciarelli et al. 2008) are as limited as those in NGC 1806, to allow final conclusions. A lack
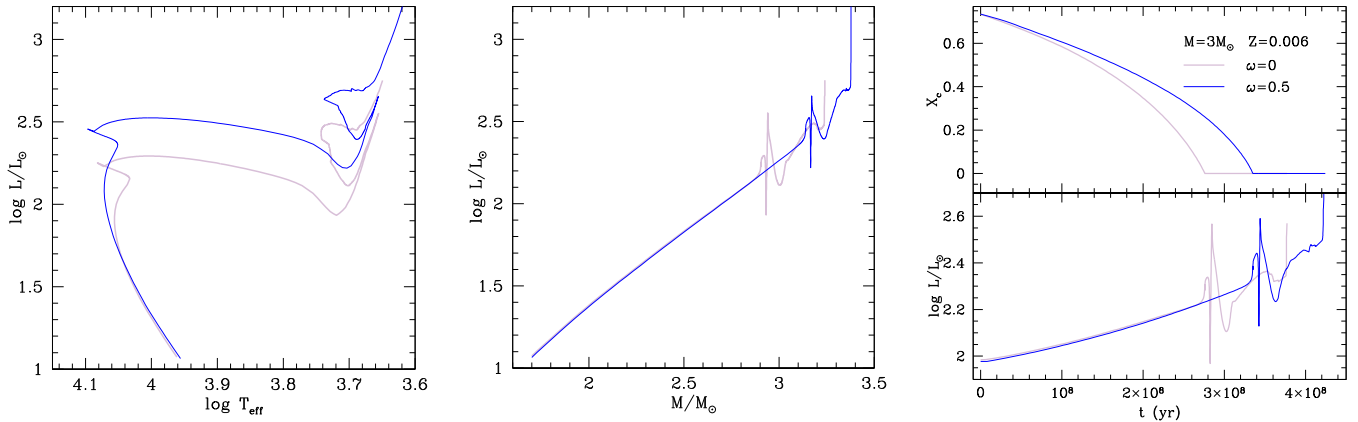
Figure 1. Left: 300 Myr isochrones for $Z = 0.006$ from Georgy et al. (2013) for non-rotating models (grey line) and models rotating at $\omega = 0.5\omega_{crit}$ (blue line); centre: luminosity versus mass for the same isochrones; right-hand side: time evolution of the 3 $M_\odot$ non-rotating and rotating models.

of the Na–O anticorrelation would call into question any attempt to use observations of the eMSTO young and intermediate-age clusters, to rule out formation and self-enrichment models for old GCs.

Bastian & de Mink (2009) suggested that stellar rotation may cause the eMSTO, as stellar rotation affects the structure of the star and the inclination angle of the star relative to the observer will change the effective temperature, hence observed colour. This result has been subsequently questioned (e.g. Girardi et al. 2011) with a number of studies supporting the idea that an age spread is responsible for the observed CMD features (Goudfrooij et al. 2011; Rubele et al. 2013). Yang et al. (2013) emphasized that the evolution of rotating models drastically depends on the parameters adopted in the description of the rotational mixing, so that the eMSTO can be explained – or not – depending on which set of models are adopted. More recently, Bastian & Niederhofer (2015) and Li, de Grijs & Deng (2014) excluded age spreads in intermediate-age LMC clusters, by inspection of their subgiant branch morphology, but their analysis was challenged by a very careful study by Goudfrooij et al. (2015). At the same time, Brandt & Huang (2015) studied the turn-off spread expected on the basis of a rotation dispersion in the component stars based on the Geneva data base created by C. Georgy and S. Ekström[1] (Georgy et al. 2014) and showed that, in the CMD of the typical *HST* bands m_{F435W} versus colour $m_{F435W} - m_{F814W}$, the turn-off area covered by turn-off stars increases, reaching a maximum towards 1–1.5 Gyr, which are in fact the typical ages of clusters with eMSTO.

In this paper, we focus our attention to the LMC cluster NGC 1856, which is much younger than any other cluster with evident eMSTO. The eMSTO has been recently identified by Correnti et al. (2015) and Milone et al. (2015) who showed that this feature is consistent with an age spread of ~80–150 Myr, although they do not exclude the rotational interpretation.

Interestingly, in addition to the eMSTO, this cluster exhibits a *split upper main sequence* which is clearly visible when the *F*336*W* filter is used (like in the m_{F555W} versus $m_{F336W} - m_{F555W}$ CMD). In a preliminary attempt dealing with models with age spread, Milone et al. (2015) show that this feature may be explained by models in which the stars belonging to the cooler main sequence (MS) have a larger metallicity. While helium and light element variations are responsible for the MS splitting observed in the old galactic GCs, their effect on the double MS of NGC 1856 has been not yet

investigated. In this paper, by using the Geneva data base, we show that the main cluster features can be interpreted in the framework of the rotational hypothesis, and provide a possible explanation for the split MS.

2 MODELS

The rotational interpretation of the extended turnoffs is linked to the initial distribution of the cluster stars' rotational velocities. Taking as an example the nominal age of 300 Myr attributed to NGC 1856 by Milone et al. (2015), the turn-off stars have mass of about 3 $M_\odot$, so the hydrogen core burning phase is convective. The evolution of stars having a convective core in the MS is dramatically affected by rotation. In fact, the mechanism of chemical mixing associated with the transfer of angular momentum from the (more rapidly rotating) convective core to the stellar envelope provides fresh hydrogen to the burning core, and extends the MS phase. Fig. 1 illustrates the difference in the isochrone location for an age of 300 Myr and metallicity $Z = 0.006$, having no rotation or a rotation equal to 0.5 the critical rotation rate (Georgy et al. 2013). The turn-off is more luminous by ~0.3 dex. The masses in evolution at the turn-off are ~2.9 $M_\odot$ in the non-rotating case, and ~3.2 $M_\odot$ for model rotating 0.5 ω_{crit} (central panel of Fig. 1). This example clearly illustrates how a range of rotational velocities in a population of coeval stars can be characterized by a broad range of turn-off luminosities and evolving masses, similar to those one would find in a cluster with non-rotating stars spread over a range of ages. The hydrogen consumption and the luminosity evolution versus time are shown in the right-hand panel of Fig. 1, for the 3 $M_\odot$ evolution. This panel makes clear that the time–luminosity evolution will depend on the detailed assumptions made concerning the mechanisms of chemical mixing.[2]

---

[1] http://obswww.unige.ch/Recherche/evoldb/index/

---

[2] These will be due both to the assumptions on rotational mixing, and to the form of overshooting of the convective core, adopted independently from rotation (that is, valid also in non-rotating models). In the stellar models used for this study, the overshoot has been parametrized so that the convective core is extended by 0.1 H_P for stars more massive than 1.7 $M_\odot$, 0.05 H_P for stars between 1.25 and 1.5 $M_\odot$ and none below. This calibration has been made for the rotating models to reproduce the width of Galactic open clusters (see Ekström et al. 2012). Non-rotating models use the same calibration for the overshoot. Thus the differences seen in Fig. 1 results only from the effect of rotational mixing.
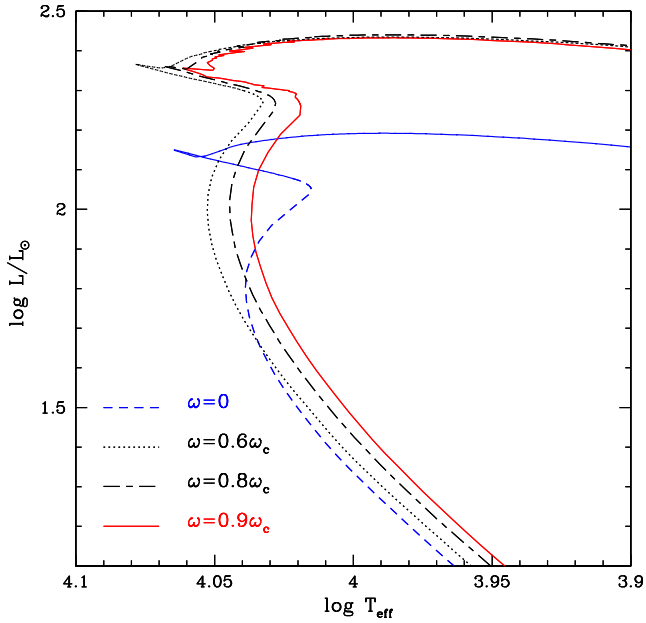
Figure 2. Comparison of isochrones in the theoretical HR diagram, for age 350 Myr, $Z = 0.006$ and different stellar angular velocity. Looking at the MSs, from left to right we have, in units of ω_{crit}, $\omega = 0$ (dashed blue), 0.6 (dotted black), 0.8 (double dashed black) and 0.9 (full line red).

It is therefore important to keep in mind that the detailed relation between turn-off spreads and rotation rates needed to model the observed CMD features depends on the specific parameters adopted in the stellar models used; a smaller rotation rate range would be needed if, for example, a higher chemical mixing efficiency than adopted in these specific models were assumed. In particular, in

the Geneva data base we use, the turn-off luminosity is not linearly related with the rotation velocity assumed for the stars, while the effect of rotation of the MS T_{eff} is. We show this in Fig. 2, where isochrones of age $t = 350$ Myr are compared for $\omega/\omega_{crit} = 0, 0.6, 0.8$ and 0.9 in the theoretical plane. We see that a significantly cooler MS requires adopting a very large rotation. This effect is increased in the observational plane by the corrections due to limb and gravity darkening.

3 THE CMD OF NGC 1856: COMPARISON WITH ROTATING MODELS

Fig. 3 shows the CMD of the cluster NGC 1856 in m_{F555W} versus the $m_{F336W} - m_{F555W}$ colour observed by Milone et al. (2015) (left-hand panel) and m_{F438W} versus $m_{F438W} - m_{F814W}$ colour (right-hand panel). Fig. 4 shows the Hess diagram in the $m_{F336W} - m_{F555W}$ colour. This is the first evidence of an eMSTO ($\gtrsim 1$ mag) in a young cluster in the Magellanic Clouds as discussed by Milone et al. (2015) and Correnti et al. (2015).

In Fig. 4, note also the split of the upper MS into two components, which host ~33 per cent and 67 per cent of MS stars in the red and blue part, respectively. The detailed analysis of Milone et al. (2015) has demonstrated that both the split of MS and the eMSTO cannot be due to photometric errors, differential reddening or unresolved binaries. The authors show that if the stars in NGC 1856 are chemically homogeneous and the eMSTO is due to a prolonged star formation, the star formation must have lasted about 150 Myr (not necessarily in a continuous way).

As discussed in Section 2, a range of stellar rotation velocities can mimic an age spread; here we show which distribution of rotational velocities is needed to reproduce the eMSTO and of the split of the upper MS.
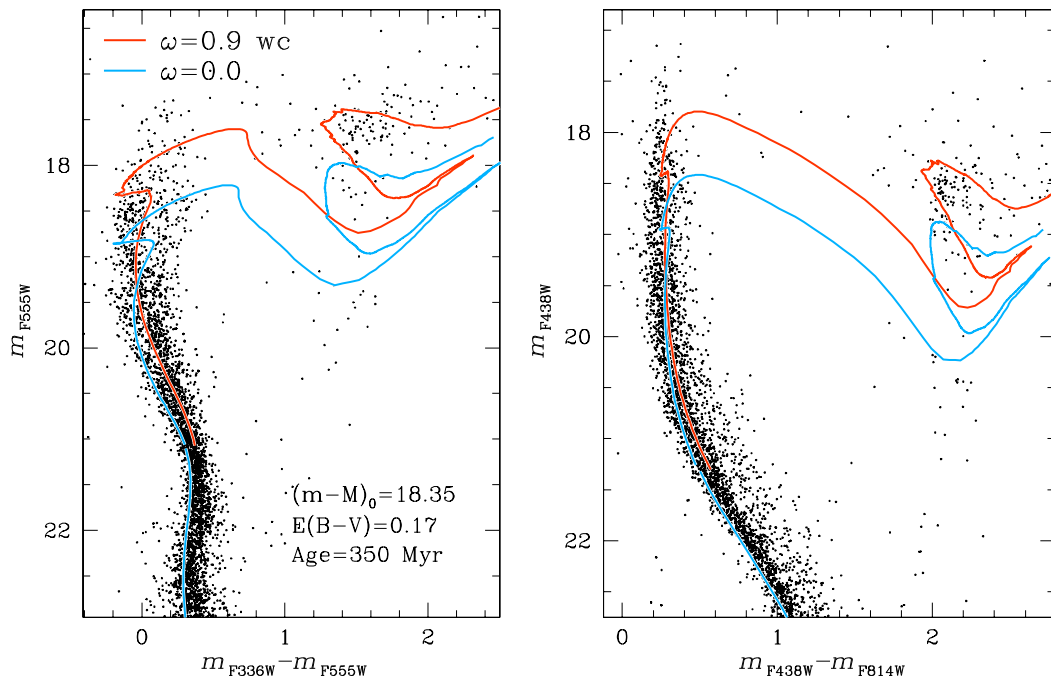

Figure 3. Two isochrones of 350 Myr for $Z = 0.006$, used for the final simulation shown in Fig. 4, are overimposed to the data from Milone et al. (2015). The left-hand panel shows the m_{F555W} versus $m_{F336W} - m_{F555W}$, and the right-hand panel shows the m_{F555W} versus $m_{F438W} - m_{F814W}$ CMDs. Two different values of angular velocities ($\omega = 0.9 \times \omega_{crit}$ and $\omega = 0$) are plotted. The non-rotating isochrone is prolonged towards low masses using the models by Mowlavi et al. (2012). This allows us to choose the value of distance modulus and reddening, labelled in the figure. The absorptions adopted in the different bands are $A_{336W}/E(B - V) = 5.10$, $A_{438W}/E(B - V) = 4.18$, $A_{555W}/E(B - V) = 3.27$, $A_{814W}/E(B - V) = 1.86$ from Milone et al. (2015).
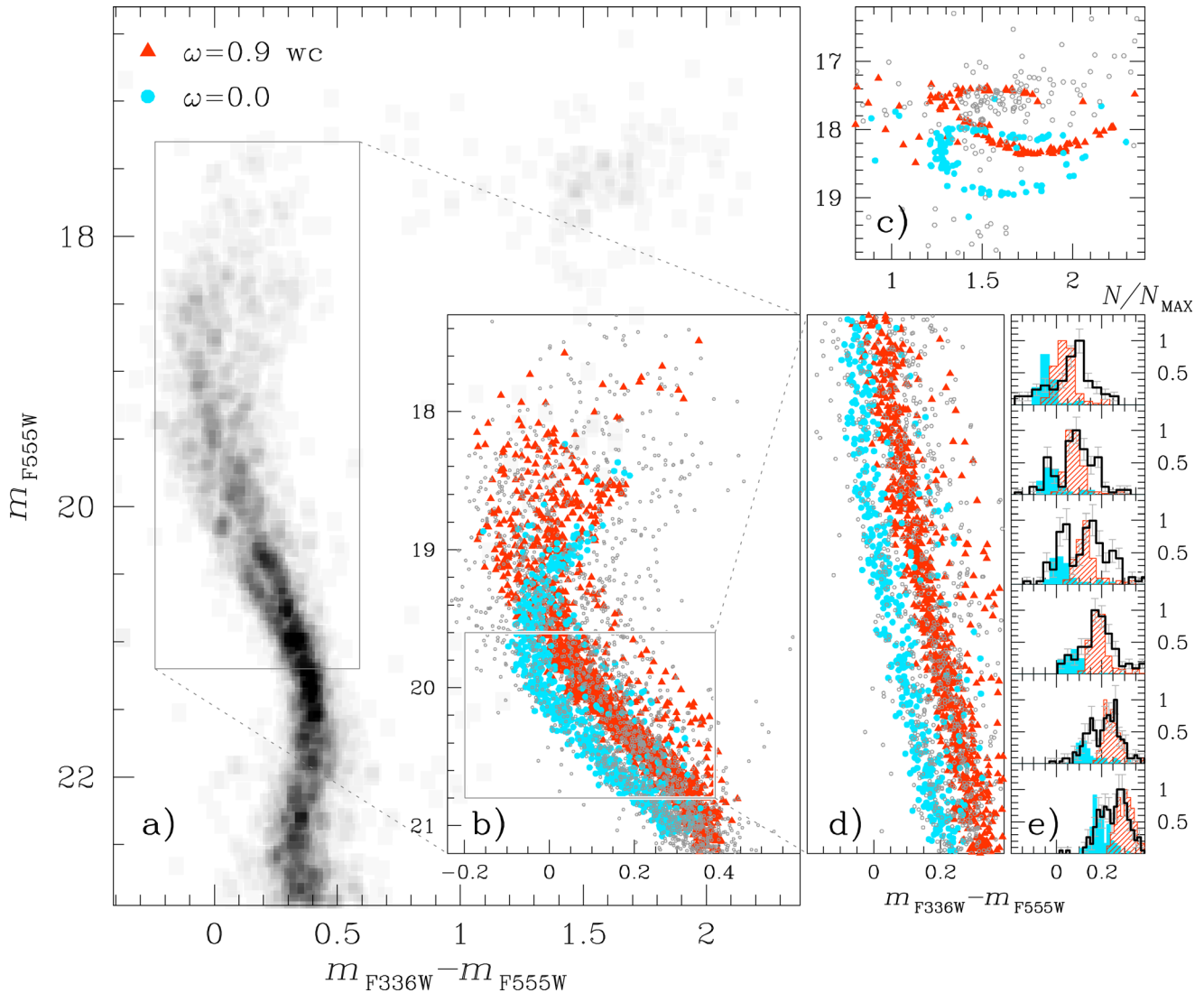
Figure 4. m_{F555W} versus $m_{F336W} - m_{F555W}$ CMD of cluster NGC 1856 and its Hess diagram. Data (grey open circle) from Milone et al. (2015) are compared with the simulations (filled triangles) described in detail in the text, at the luminosity of the turn-off (panel b); the red clump (c); and the upper part of MS (d). For this last case, the histogram of the Δ ($m_{F336W} - m_{F555W}$) distribution for stars in six magnitude intervals is reported in panel e, after having verticalized the upper part of the MS delimited by the grey boundaries in panel b).

In Fig. 3, we show the comparison between data and rotating versus non–rotating stellar models. The isochrones, both for 350 Myr, are taken from the Geneva data base and are calculated from the models by Georgy et al. (2013). The metallicity we adopt is $Z = 0.006$, that is the metallicity available on the data base, closest to that inferred from spectroscopy (Harris & Zaritsky 2009) for the young populations of the Large Magellanic Cloud.

For the non-rotating case we extend the isochrones to the masses $M < 1.6\ M_\odot$ by means of the models published by Mowlavi et al. (2012). The extension helps to choose a suitable reddening and distance modulus, which are labelled in Fig. 3. In order to reproduce the split in the upper MS, for the selected age, the population of rotating stars must be characterized by a rotation rate close to breakup ($\omega \sim 0.9 \times \omega_{crit}$) (Fig. 3, left-hand panel). Notice that the split of MS is less evident in the colour $m_{F438W} - m_{F814W}$ (Fig. 3, right-hand panel), and the MSTO has a vertical structure. For this reason, UV photometry is crucial to shed light on the eMSTO phenomenon in NGC 1856. With this

choice of rotation and age, we then select from the data base, the corresponding synthetic photometry with a random viewing angle distribution, using the gravity darkening model by Espinosa Lara & Rieutord (2011) and including the limb darkening effect (Claret 2000). The data of the synthetic simulation were transformed into observational planes using the model atmospheres by Castelli & Kurucz (2003), convolved with the *HST* filter transmission curves.

In the simulation, we take into account the combined photometry for 30 per cent of binaries, following the procedure outlined in Milone et al. (2009). Binaries are included both in the rotating and non-rotating group. The mass function of the secondary stars is randomly extracted from a Salpeter's like mass function, with a lower limit of $0.4\ M_\odot$. Notice that only the photometric consequences of the presence of such binaries are monitored in the simulations (for the evolutionary consequences, see the discussion in Section 4.1), and that the choice for the percentage of binaries is chosen based on the estimate by Milone et al. (2015).

As shown in Fig. 4, this simulation describes well the eMSTO and the bimodality of the upper MS.

In other aspects the simulation is not completely satisfactory. In particular, it fails to reproduce the data after the end of the central H-burning phase. We suggest that this may depend both on the parametrization of the overshoot in the Geneva models and on the way in which the luminosity and temperature are corrected for the inclination angle (see also discussion in Section 4.1).

The simulation fails also to reproduce the red clump (panel c in Fig. 4), but for a possible solution of this problem see Section 4.1.

4 DISCUSSION

4.1 General adequacy of rotating models

The results shown in the panels of Fig. 4 rely on the Geneva data base, and should be considered as a first attempt to explain the eMSTO and the split upper MS in NGC 1856 in terms of differences in the rotational velocities of stellar subsets. Noticeably, the Geneva data base was built before the recent discoveries on NGC 1856 and it is remarkable how the models do such a good job in reproducing its split MS.

There are two incomplete issues in the synthetic models: first, the red side of the eMSTO region is not well reproduced. It looks like the end of core hydrogen burning is not as sharply defined in reality as it occurs in the models we have used. This looks plausible, as the rotation and mixing issue may be subject to several minor second-order parameters which cannot easily be taken into account in modelling. Secondly, the splitting of the MS is best reproduced if we assign a very fast rotation ($\omega = 0.9\omega_{\text{crit}}$) to the numerous sample (67 per cent of stars) defining the redder MS and the upper turn-off. This may depend on the way gravity and limb darkening are introduced in the models. This is the first adequate representation of the splitting, so it is a powerful hint that rotation is the reason for the CMD features, even if we should not take the very high rotation at face value.

Alternatives to the rotational interpretation can reside in different metallicity, or different specific elemental abundances for the two sides of the MS, but further modelling is required, and whether such differences exist, should be checked by future spectroscopic observations.

The final problem is that the clump reproduction is quite modest. While the rotating simulation reproduces the luminosity location of the clump, there should be a second clump (less populated) about 1 mag dimmer, but the data do not show it. The clump evolution is a very delicate issue, the ratio of blue to red stars depending on the detailed treatment of convection and mixing. Consideration of non-instantaneous mixing produces favours a long evolution in the blue side of the clump (e.g. Ventura, Castellani & Straka 2005), so it could describe better the clump here. Here again, notice that age differences produce a similar problem for the clump(s) location. A possible solution of this problem occurs naturally if the slow-rotating stars are all binaries, as discussed in Section 4.2. Observational data and theoretical considerations show that orbital periods between 4 and 500 d can be effective in producing slow stellar rotation (Abt & Boonyarak 2004). As we are dealing with evolving masses ∼3 M$_\odot$, orbital periods between ∼50 and 500 d, according to Kepler's law, would produce Roche lobe interaction and mass transfer from the primary star while it is evolving along the red giant branch. Shorter periods produce mass transfer at an earlier phase, during the crossing of the Hertzsprung gap. Thus the evolving star would not reach helium ignition as a single star

would, and the low luminosity blue hook could result depopulated. In the end, the lack or sparseness of a low-luminosity clump might lend further support to the hypothesis of a rotational origin for the splitting of the turn-off.

A consequence of this interpretation is that the role of binaries in the CMD should be reconsidered. The slowly rotating group should be made of 100 per cent binaries with periods between 4 and 500 d, while the rapidly rotating group would include both single stars and longer period binaries. The binaries clearly seen on the right of the observed MS(s) could be mostly belonging to the non-rotating population. A full discussion of this problem goes beyond the purpose of this work, and is delayed to a following investigation.

4.2 Why two populations?

Our analysis has shown that in order to reproduce the observed features of the CMD of NGC 1856, it is necessary to have a large fraction of cluster stars (2/3) retaining the large rotational velocity typical of the B and A stars (see e.g. Zorec & Royer 2012, for A-type stars), while the remaining 1/3 of the stars must have slowed down early enough to prevent rotational mixing, and have evolved as standard non-rotating or slowly rotating models.

The key question to address therefore concerns the mechanism and processes responsible for slowing down a large fraction of stars during the H-core burning evolution.

Zorec & Royer (2012) have gathered and analysed the rotational velocities of fields A-type MS stars (types B6 to F2). They found that stars below 2.5 M$_\odot$ show an unimodal velocity distribution displaying a small acceleration as the stars evolve along the MS. On the contrary, stars between 2.4 and 3.85 M$_\odot$ display a clear bimodal distribution with a slow velocity component (up to 20 per cent for the 2.8 M$_\odot$ bin). They found that the two peaks are clearly separated during the MS evolution but these peaks tend to bend near the turn-off. This dichotomy in velocity persists if close binary and chemically peculiar stars are included. The origin of the slow component is unknown but the authors make two hypotheses: (1) some stars have already lost all their angular momentum during the pre-MS due to magnetic braking or (2) in a fraction of undetected binaries, tidal interactions have slowed down the stars. It should also be noted that a similar bimodality in the velocity distribution have been detected among early B-type stars by Dufton et al. (2013).

Abt & Boonyarak (2004), in a study of the velocities of A- and B-type binaries, found that close binaries (period smaller than 4 d) are all synchronized and circularized. Binaries with period longer than 500 d display the same rotational properties as single stars. For binaries with period between 4 and 500 d, rotational velocity is significantly smaller than for single stars, with about one-third to two-third of their angular momentum being lost, presumably, by tidal interactions.

On the theoretical side, tides in binaries will be responsible to the synchronization and circularization of the orbit (Zahn 1977). For low-mass stars with a convective envelope, the main mechanism is the viscous dissipation of the kinetic energy acting like an equilibrium tide. On the other hand, in more massive stars with a convective core, some low-frequency modes of oscillation can be excited by the periodic tidal potential. The response to this excitation is called the dynamical tide (see e.g. Kopal 1968). With a simplified model, assuming an uniform rotation, Zahn (1977) obtains the following expression for the synchronization time:

$$\frac{1}{t_{\text{sync}}} = 5 \times 2^{5/3} \left(\frac{GM}{R^3}\right)^{1/2} q^2 (1+q)^{5/6} \frac{MR^2}{I} E_2 \left(\frac{R}{a}\right)^{17/2}, \quad (1)$$

where q is the mass ratio of the binary, E_2 is the parameter measuring the coupling between the tidal potential and the gravity mode which depends on the convective core mass ($\sim 5 \times 10^{-8}$ for a 3 $M_\odot$). Zahn (2008) shows that the synchronization time scales with $(I/MR^2)/E_2R^7$, which increases during the MS. Thus, we can conclude that most of the tidal interaction will take place around the zero-age main sequence, so that binaries dispersion, if it occurs during the MS, will take place in systems already slowed-down. Moreover, early-type binaries have their transition period (for circularization), observed through OGLE and MACHO gravitaional microlensing surveys, well in agreement with the dynamical tides theory (North & Zahn 2003). However, an important fraction of binaries are also circularized even if the semimajor axis is larger. This may indicate that another more efficient mechanism is at play for them. One possibility will be that these binaries have undergone several episodes of resonance locking (see Witte & Savonije 1999a,b, for the effect on a 10 $M_\odot$ primary)

In summary, there are several ways to slow down a fraction of the cluster stars (see also the extended discussion in Dufton et al. 2013). If we look into more detail into the binary hypothesis, we should expect that most of the non-rotating stars hide a binary companion. In fact, binaries of periods in the range 4–500 d would be hard binaries in the core of this cluster, whose central dispersion velocity is ~ 2.5 km s^{-1} (McLaughlin & van der Marel 2005). Only binaries with period longer than $\sim 10^3$ yr would be ionized in the central regions. Notice that the cluster seems to host ~ 30 per cent (Milone et al. 2015) of binaries, so this hypothesis is not unreasonable. Further investigations may provide further insight into this problem.

4.3 The case of multiple populations in old globular clusters

We conclude our discussion with some comments and cautionary remarks about the connection between eMSTO clusters and multiple-population old GCs.

Evidence of multiple populations in old GCs comes from an extensive number of photometric and spectroscopic studies showing that stars in old GCs are characterized by a spread in the abundances in helium and light elements (such as Na, O, Mg, Al). Photometric studies have also shown the widespread presence of discrete groups with distinct photometric properties corresponding to different chemical properties (see e.g. Piotto et al. 2015). These are the key fingerprints of multiple populations in old GCs and provide the main constraints for any theoretical effort aimed at modelling the formation history of these systems and shedding light on the source of processed gas composing the second-generation populations observed in GCs.

While the study of young and intermediate-age clusters (hereafter YICs) might provide some clues to the answers to the many questions raised by the discovery of multiple populations in old GCs, it is important to exercise much caution in connecting YICs and old GCs for this purpose and in drawing conclusions about different theoretical scenarios for the formation of old GCs from observations of YICs.

Some specific issues to consider are the following.

(1) It is not clear whether the YICs studied so far actually host multiple populations at all. As mentioned in the Introduction, for example, a spectroscopic study of one of the eMSTO clusters (NGC 1806) does not reveal the typical chemical fingerprints of multiple populations found in old GCs. Photometric signatures which might be ascribed to extended star formation history in YICs,

such as those discussed in this and other works, have possible alternative explanations unrelated to the presence of multiple stellar populations with different chemical properties. It is important to realize that spectroscopic characterization of YIC aimed at shedding light on the presence of (or the lack of) the chemical patterns typical of multiple populations is desirable to make a solid connection between YIC and old multiple-populations GCs even if strong evidence of an age spread in YIC were to be established. Although, as remarked in Section 1, many additional spectroscopic studies are necessary to clarify this issue, it is possible that the study of these clusters might be irrelevant to shed light on the formation history of multiple-population old GCs.

(2) While eMSTO, as also argued in this paper, might indeed be explained without relying to extended periods of star formation (and eMSTO clusters might not host chemically different multiple populations), studies ruling out star formation episodes extending for a few hundred Myr (see e.g. Bastian & Silva-Villa 2013; Bastian et al. 2013) have been presented as evidence against the asymptotic giant branch (AGB) scenario of multiple-population formation. We point out here that in all the studies (see e.g. D'Ercole et al. 2008, 2010, 2012) aimed at modelling the chemical properties of multiple-population old GCs using AGB ejecta, the epoch of second-generation formation is limited to a time interval between about 30 and 100 Myr with a significant fraction of second-generation stars forming in the early phase of this period. While in a few clusters second-generation star formation might have extended beyond (see e.g. D'Antona et al. 2011) the current observational constraints from spectroscopic studies – in particular the lack of C+N+O increase in the second-generation stars of most clusters – do not, in general, allow such an extended period of second-generation star formation. In addition to urging caution in connecting YICs and old GCs, it is important to realize that lack of evidence of such an extended age spread cannot be used as evidence against AGB models.

(3) Finally, we emphasize the importance of properly considering the differences between the structural properties of YIC and old GCs. The current properties of old GCs have been affected by early and long-term evolutionary processes (e.g. gas expulsion, mass-loss due to stellar evolution, two-body relaxation, tidal interactions). Reconstructing their structure and mass at the time of second-generation formation in order to identify the threshold in the structural properties allowing the formation of multiple populations is not a trivial task. Identifying young clusters with present masses similar to the current masses of old multiple-population clusters to test multiple-population formation scenarios, without considering the complications of properly reconstructing the evolutionary history of old GCs, may easily lead to erroneous conclusions. For example the current mass of NGC 1856 is about 10^5 $M_\odot$ (McLaughlin & van der Marel 2005), similar to the current mass of some old GCs hosting multiple populations. Its structural properties are such the central escape speed is about 10 km s^{-1} (McLaughlin & van der Marel 2005). Detailed models would be necessary to understand whether initial/earlier properties allowing the formation of a significant fraction of second-generation stars are among those evolving into NGC 1856's current properties – see Correnti et al. (2015) for an attempt to address this issue; see also Goudfrooij et al. (2014). However, the current structural properties, if sufficiently similar to those of the cluster at earlier stages of its life, would indicate that this cluster is not capable to retain a significant fraction of the ejecta of AGB or other possible sources of processed gas, lend support to the interpretation of the eMSTO in terms of different rotational

velocities, and provide an example of the caution necessary in using these stellar systems to draw any conclusion about multiple population formation models.

REFERENCES

Abt H. A., Boonyarak C., 2004, ApJ, 616, 562
Bastian N., de Mink S. E., 2009, MNRAS, 398, L11
Bastian N., Niederhofer F., 2015, MNRAS, 448, 1863
Bastian N., Silva-Villa E., 2013, MNRAS, 431, L122
Bastian N., Cabrera-Ziri I., Davies B., Larsen S. S., 2013, MNRAS, 436, 2852
Brandt T. D., Huang C. X., 2015, ApJ, 807, 25
Carretta E., Bragaglia A., Gratton R., Lucatello S., 2009, A&A, 505, 139
Castelli F., Kurucz R. L., 2003, in Piskunov N., Weiss W. W., Gray D. F., eds, Proc. IAU Symp. 210, Modelling of Stellar Atmospheres. Astron. Soc. Pac., San Francisco, p. 20P
Claret A., 2000, A&A, 363, 1081
Conroy C., Spergel D. N., 2011, ApJ, 726, 36
Correnti M., Goudfrooij P., Puzia T. H., de Mink S. E., 2015, MNRAS, 450, 3054
D'Antona F., D'Ercole A., Marino A. F., Milone A. P., Ventura P., Vesperini E., 2011, ApJ, 736, 5
D'Ercole A., Vesperini E., D'Antona F., McMillan S. L. W., Recchi S., 2008, MNRAS, 391, 825
D'Ercole A., D'Antona F., Ventura P., Vesperini E., McMillan S. L. W., 2010, MNRAS, 407, 854
D'Ercole A., D'Antona F., Carini R., Vesperini E., Ventura P., 2012, MNRAS, 423, 1521
Dufton P. L. et al., 2013, A&A, 550, A109
Ekström S. et al., 2012, A&A, 537, A146
Espinosa Lara F., Rieutord M., 2011, A&A, 533, A43
Georgy C., Ekström S., Granada A., Meynet G., Mowlavi N., Eggenberger P., Maeder A., 2013, A&A, 553, A24
Georgy C., Granada A., Ekström S., Meynet G., Anderson R. I., Wyttenbach A., Eggenberger P., Maeder A., 2014, A&A, 566, A21
Girardi L., Eggenberger P., Miglio A., 2011, MNRAS, 412, L103
Goudfrooij P., Puzia T. H., Chandar R., Kozhurina-Platais V., 2011, ApJ, 737, 4
Goudfrooij P. et al., 2014, ApJ, 797, 35
Goudfrooij P., Girardi L., Rosenfield P., Bressan A., Marigo P., Correnti M., Puzia T. H., 2015, MNRAS, 450, 1693
Gratton R. G., Carretta E., Bragaglia A., 2012, A&AR, 20, 50
Harris J., Zaritsky D., 2009, AJ, 138, 1243
Kopal Z., 1968, Ap&SS, 1, 179
Li C., de Grijs R., Deng L., 2014, Nature, 516, 367
Mackey A. D., Broby Nielsen P., Ferguson A. M. N., Richardson J. C., 2008, ApJ, 681, L17
McLaughlin D. E., van der Marel R. P., 2005, ApJS, 161, 304
Milone A. P., Bedin L. R., Piotto G., Anderson J., 2009, A&A, 497, 755
Milone A. P. et al., 2015, MNRAS, 450, 3750
Mowlavi N., Eggenberger P., Meynet G., Ekström S., Georgy C., Maeder A., Charbonnel C., Eyer L., 2012, A&A, 541, A41
Mucciarelli A., Carretta E., Origlia L., Ferraro F. R., 2008, AJ, 136, 375
Mucciarelli A., Dalessandro E., Ferraro F. R., Origlia L., Lanzoni B., 2014, ApJ, 793, L6
North P., Zahn J.-P., 2003, A&A, 405, 677
Piotto G. et al., 2012, ApJ, 760, 39
Piotto G. et al., 2015, AJ, 149, 91
Rubele S., Girardi L., Kozhurina-Platais V., Kerber L., Goudfrooij P., Bressan A., Marigo P., 2013, MNRAS, 430, 2774
Ventura P., Castellani M., Straka C. W., 2005, A&A, 440, 623
Witte M. G., Savonije G. J., 1999a, A&A, 341, 842
Witte M. G., Savonije G. J., 1999b, A&A, 350, 129
Yang W., Bi S., Meng X., Liu Z., 2013, ApJ, 776, 112
Zahn J.-P., 1977, A&A, 57, 383
Zahn J.-P., 2008, in Goupil M.-J., Zahn J.-P., eds, EAS Publ. Ser. Vol. 29, Tidal Effects in Stars, Planets and Disks. EDP Sciences, Les Ulis, p. 67
Zorec J., Royer F., 2012, A&A, 537, A120

This paper has been typeset from a TEX/LATEX file prepared by the author.